Sains Malaysiana 55(2)(2026): 245-255
*http://doi.org/10.17576/jsm-2026-5502-05*

# Fabrication of Lead(II) Ion-Selective Electrode (Pb-ISE) Based on Photopolymerization of Metyl Methacrylate-Tetrahydrofurfuryl Acrylate (MT) Copolymer Thin Films

(Fabrikasi Elektrod Pemilih Ion Plumbum(II) (Pb-ISE) Berasaskan Fotopempolimeran Filem Nipis Kopolimer Metil Metakrilat-Tetrahidrofufuril Akrilat (MT))

SAGIR ALVA[1,*], I GUSTI AYU ARWATI[1], MUHAMMAD FITRI[1], RITA SUNDARI[1], IRWANA NAINGGOLAN[2,3] & TULUS IKHSAN NASUTION[4]

[1]*Mechanical Engineering Department, Faculty of Engineering, Universitas Mercubuana, Jl. Meruya Selatan No 1, West Jakarta- Jakarta, Indonesia, 11650*
[2]*Department of Chemistry, Faculty of Mathematics and Natural Science, Universitas Sumatera Utara, Medan, 20155, Sumatera Utara, Indonesia*
[3]*Center of Excellent Chitosan and Advance Materials, Universitas Sumatera Utara, 20155, Medan, Indonesia*
[4]*Department of Physics, Faculty of Mathematics and Natural Science, Universitas Sumatera Utara, Medan 20155, Sumatera Utara, Indonesia*

*Received: 21 September 2024/Accepted: 24 January 2026*

## ABSTRACT

The fabrication of lead(II)-ion selective electrode (Pb-ISE) that uses a methyl methacrylate (MMA)-tetrahydrofurfuryl acrylate (THFA) copolymer membrane, known as MT, was successfully done. In this study, MT copolymer membranes were fabricated using a photopolymerization technique with an optimal ratio of MMA: THFA of 2:8 (MT28). The diffusion coefficient of MT 28 copolymer was $1.05 \times 10^{-8}$ cm$^2$/s and the Nernstian number value was 27.2 mV/dec. Furthermore, the linear range produced by Pb-ISE using MT28 ranges from 0.1 to $10^{-6}$ M and has a limit detection (LoD) value of $5.37 \times 10^{-7}$ M. The selectivity coefficient test ($\text{LogK}^{\text{pot}}_{a,b}$) was carried out using separated solution methods (SSM) on five interfering ions consisting of $K^+$, $Na^+$, $Mg^{2+}$, $Cd^{2+}$, and $Cu^{2+}$. The $\text{LogK}^{\text{pot}}_{a,b}$ values obtained respectively were -6.64 ± 0.14, -6.10 ± 0.07, -12.20 ± 0.16, -6.07 ± 0.15 and -4.23 ± 0.17. The Pb-ISE based on MT28 copolymer has a working area at pH 3-9 and also shows the same good performance as testing using standard $Pb^{2+}$ ion measurements using Atomic Absorption Spectroscopymetry (AAS) referring to SNI 06–6989.8-2004.

Keywords: Lead (II); ion-selective electrode; photopolymerization; methyl methacrylate; tetrahydrofurfuryl acrylate

## ABSTRAK

Fabrikasi elektrod pemilih ion plumbum(II) (Pb-ISE) yang menggunakan membran kopolimer metil metakrilat (MMA)-tetrahidrofurfuril akrilat (THFA) atau dikenali sebagai MT telah berjaya dijalankan. Membran kopolimer MT telah difabrikasi menggunakan kaedah fotopempolimeran dengan nisbah optimum MMA:THFA 2:8 (MT28). Pekali resapan kopolimer MT 28 yang diperoleh ialah $1.05 \times 10^{-8}$ cm$^2$/s dan nilai nombor Nernstian ialah 27.2 mV/dec. Tambahan pula, julat linear yang dihasilkan oleh Pb-ISE menggunakan MT28 adalah antara 0.1 hingga $10^{-6}$ M dan mempunyai nilai pengesanan had (LoD) $5.37 \times 10^{-7}$ M. Ujian pekali pemilihan ($\text{LogK}^{\text{pot}}_{a,b}$) telah dijalankan menggunakan kaedah larutan terpisah (SSM) ke atas lima ion gangguan yang terdiri daripada $K^+$, $Na^+$, $Mg^{2+}$, $Cd^{2+}$ dan $Cu^{2+}$. Nilai $\text{LogK}^{\text{pot}}_{a,b}$ yang diperoleh masing-masing ialah -6.64 ± 0.14, -6.10 ± 0.07, -12.20 ± 0.16, -6.07 ± 0.15 dan -4.23 ± 0.17. Pb-ISE berasaskan kopolimer MT28 mempunyai kawasan kerja pada pH 3-9 dan juga menunjukkan prestasi baik yang sama seperti ujian menggunakan kaedah piawai Spektroskopi Penyerapan Atom (AAS) untuk ion $Pb^{2+}$ merujuk kepada SNI 06–6989.8-2004.

Kata kunci: Elektrod pemilih ion; metil metakrilat; pemfotopolimeran; plumbum(II); tetrahidrofurfuril akrilat

## INTRODUCTION

Lead(Pb) is a heavy metal that has a wide range of applications, and it is commonly found in the form of divalent ions or $Pb^{2+}$ (Zheng et al. 2014). This metal is commonly utilized in the battery, paint, pipe, chemical, and electronics industries, and it can also be observed naturally in the oil and gas industry (Alva et al. 2019; Fijalkowska, Karpisz & Wisniewska 2020; Ghoochani et al. 2023; Hardi et al. 2019; Iqbal, Jan & Shah 2021; Megarajan, Kanth & Anbazhagan 2020; Wodyk et al. 2023). Monitoring the presence of Pb metal in water and the environment is necessary since it is a toxic metal. Lead metals can enter the body through different pathways such as through the food chain, respiration, or absorption through the skin. The accumulation of heavy metals in the body can lead to damage to vital organs like the liver, brain, nervous system, and spine. Several deaths have occurred in the oil and gas industry due to all of these conditions (Gordo et al. 2021). The WHO recommends that the amount of Pb metal in acceptable concentrations should not exceed 10 ppb (Alva et al. 2024; Ariri et al. 2022; Megarajan, Kanth & Anbazhagan 2020).

In general, $Pb^{2+}$ ions in a sample have been analyzed by several instruments. Some of the equipment mentioned include UV-Vis spectrophotometry (Yagmuroglu 2023), AAS (Karatepe et al. 2022), ICP-OES (Smirnova, Mikheev & Apyari 2024), chromatography (Muhammad et al. 2020) and electrophoresis (Li et al. 2016). However, these devices tend to be large, making them difficult to use for direct measurement applications in the field. This situation makes it difficult to produce information on the presence of $Pb^{2+}$ ions in the field quickly. Furthermore, this equipment generally necessitates significant and complicated operational expenses. Alternatively, $Pb^{2+}$ ion measurements can also be performed using a chemical sensor (Udos et al. 2023; Wang et al. 2023; Yang et al. 2023).

A chemical sensor is a device that converts chemical information into easily recognizable electrical signal information when a target chemical is present in a sample (Baranwal et al. 2022). Chemical sensors have played a significant role in a variety of areas, including industrial processes, environment, health, agriculture, fisheries, military, and many other areas (Li et al. 2023; Saleh & Fadillah 2023). Chemical sensors have several advantages over the devices mentioned in the paragraph earlier. Some of the advantages of chemical sensors include the fact that they can be fabricated in small sizes, so they can be used easily. Therefore, the information generated can be faster. Additionally, chemical sensors are simple to operate and do not require many samples (Arakawa, Dao & Mitsubayashi 2022).

The ion selective electrode (ISE) is an interesting chemical sensor that can be used to detect $Pb^{2+}$ ions. The ISE sensor has advantages, including being widely applicable for ion sensors, simple fabrication, fast measurement response, not damage samples, a long measurement distance and is not affected by colour or turbidity (Alva et al. 2024, 2019; Ariri et al. 2022). In an ISE, the membrane layer is a vital component. This layer is the heart of the ISE sensor, and this membrane layer is very selective for the presence of target ions (Alva et al. 2020). The development of $Pb^{2+}$ sensors with ISE was done before by researchers, including Arfin and Tarrannum (2019) using iodate membranes made of Polyaniline-zirconium (IV). The sensor developed by Arfin demonstrates good performance, because it can detect concentrations as low as 2.07 ppb. However, its application is limited to measurements within a pH range of 2.5-6.5, whereas some samples have pH values exceeding 6.5. Meanwhile, Liu et al. (2021) developed an ISE Pb sensor using PANI-PFOA membrane material. Although the resulting sensor is quite stable, it can only be used to test Pb samples up to the lowest level of 207 µg/L. This value is still too far from the WHO recommendations. Meanwhile, Nisah et al. (2022) developed an ISE Pb sensor using polyurethane membranes and 1,10-phenanthroline as active agents which can measure up to 0.0207 pbb. Regrettably, the sensor only remains stable at pH 7-8, while $Pb^{2+}$ ions are more prevalent in samples with $pH<7$. So, an alternative membrane material is needed for ISE fabrication to detect $Pb^{2+}$ ions.

One of the materials that has the potential to be developed is a methylmethacrylate-tetrahydrofuryl acrylate (MT) copolymer membrane. This membrane has been applied to ISFET fabrication for nitrate ion ($NO_3^-$) detection developed by Nor Farhana et al. (2014). The $NO_3$-ISFET based on MT membranes gave quite good results. Furthermore, this MT membrane has not been utilized for ISE manufacturing of $Pb^{2+}$ ions. Therefore, this provides an opportunity to be applied in the fabrication of Pb-ISE sensors. This MT membrane has advantages such as its fabrication process being very easy, which can be provided with photopolymerization techniques. This technique can be done in a few minutes, does not require a lot of materials, can be mass-produced, and has excellent adhesion to the electrode surface. This study aims, to carry out diffusion tests on different types of MT membrane variants, adjust the MT composition, and evaluate the performance of the Pb-ISE sensor.

## MATERIALS AND METHODS

### INSTRUMENTATIONS

In this study, some of the equipment used includes an electrochemical workstation device (Corrtest CS350), 9V battery, Ag/AgCl reference electrode, 2B Graphite pencil as a counter electrode, Ag Screen Printed Electrode from Scrint-Print Sdn Bhd-Malaysia, pH meter and 80 watt UV Box Exposure.

### MATERIALS

Meanwhile, the materials used in this study include methyl methacrylate (MMA) and tetrahydrofurfuryl acrylate (THFA) monomers, 1,6-Hexanediol diacrylate (HDDA) as a cross-linker agent, 2,2-Dimethoxy-2-phenylacetophenone (DMPP) as a photoinitiator, Lead Ionophore (IV) and Potassium tetrakis(4-chlorophenyl)borate (KTpClPB) as lipophilic salts. Meanwhile, the salts used in this study include lead(II) nitrate ($Pb(NO_3)_2$), potassium chloride (KCl), magnesium chloride hexahydrate ($MgCl_2.6H_2O$), cadmium chloride hydrate ($CdCl_2.xH_2O$), potassium phosphate dibasic ($K_2HPO_4$) and potassium phosphate monobasic ($KH_2PO_4$). In addition, other materials used include sodium hydroxide (NaOH), $N_2$ gas, hydrochloride acid (HCl) and deionized water (DIW).

## EXPERIMENTS

The preparation and characterization of Ag/AgCl transducers was done by using the same procedure as Khaerudini, Rahman and Alva (2020), which involves growing an AgCl layer on the Ag-SPE surface. Next, 5 µL of a mixture of MMA and THFA monomers with the composition shown in Table 1 was deposited onto the surface of the Ag/AgCl layer. Afterwards, the photopolymer process was carried out with UV light for 180 s under $N_2$ gas flow. After the MT copolymer film layer was formed, testing was carried out on the $Pb^{2+}$ ion response by connecting the Ag/AgCl reference electrode and the SPE electrode having a MT layer to the electrochemical workstation device. Both electrodes that have been installed are then dipped into various concentrations of $Pb(NO_3)_2$ solution and the resulting mV value is recorded. Furthermore, the chronoamperometry method was used to test the diffusion coefficient. In this test, the Ag/AgCl electrode acts as a reference electrode, graphite pencil 2B as a counter electrode and SPE with MT layer acts as a working electrode. The test was conducted in a solution that contained 0.1 M $Pb(NO_3)_2$. Additionally, the most effective MT copolymer was chosen for the ionophore optimization process during the fabrication of Pb-ISE.

The ionophore optimization process was carried out by mixing the best MT mixture with variations in the mole ratio between KTpClPB and ionophore of 2:1, 1:1, 1:2, and 1:3 mole ratio. The previously prepared MT mixture was then drop cast onto the surface of the Ag/AgCl SPE and photopolymerization was carried out for 180 s under $N_2$ gas flow conditions. After the MT copolymer layer is formed, it is then hydrated with a $Pb(NO_3)_2$ solution with a concentration of 0.01 M for 20 min. After hydration, the SPE was connected to an electrochemical workstation device and its potential value was measured using a variety of concentrations of $Pb(NO_3)_2$ solution, as shown in Figure 1. Next, the obtained mV values were plotted on an x-y scatter curve, and the best copolymer composition was selected based on the best Nernstian number (Alva et al. 2024). The best Pb-ISE was then selected for performance testing including linear range, detection limit, selectivity coefficient ($LogK^{pot}_{a,b}$), pH effect, life span, and validation testing using AAS.

## RESULTS AND DISCUSSION

### OPTIMIZATION OF MT COPOLYMER COMPOSITION

The presence of a membrane layer in the fabrication of an ISE like Pb-ISE is of great importance (Alva et al. 2024). The ability of an ISE to respond to the presence of target ions also depends greatly on the membrane's ability to allow target ions to diffuse from the sample phase into the membrane phase (Alva et al. 2019). Therefore, it is important to conduct a study on the effect of diffusion coefficient on the variation of MT copolymer composition in this study. This cannot be separated from the characteristics of poly(methyl methacrylate) (PMMA), which has a higher glass transition temperature ($T_g$) value than poly(tetra hydrofurfuryl acrylate) (pTHFA) (Alva et al. 2020; Hajduk et al. 2021). In the end, the flexibility and diffusion coefficient of the MT copolymer provided will be affected by the differences in $T_g$ values between PMMA and PTHFA. This diffusion coefficient test was conducted in a $Pb(NO_3)_2$ solution containing 0.1 M over a 60 s using the chronoamperometry method. The test results can be seen in Figure 2.

According to Figure 2, the more MMA components there are in the MT co-polymer, the less $Pb^{2+}$-ions can diffuse. This can be seen from the t1/2 peak (30 s) for the copolymer with the MMA: THFA ratio (40:60 w/w, yellow line) which is very low compared to the other three ratios. Furthermore, it can be observed that MT46 exhibits the lowest diffusion coefficient value, which is determined using the Cottrell equation (Yevgeniya et al. 2020). This is also confirmed by the results of potentiometric testing of $Pb(NO_3)_2$ solution with concentration variations of 0.1 – $10^{-8}$ M as seen in Figure 3 and Table 2.

Based on the data from Figure 3 and Table 2, it can be seen that the MT copolymer with a ratio of 19 has the largest diffusion rate of $1.51 \times 10^{-8}$ cm²/s. However, the resulting Nernstian number is super-Nernstian ( > 34.6 mV/dec), where the ideal Nernstian number for a two-charged ion such as $Pb^{2+}$ ion is 29.6 ± 5 mV/dec (Alva et al. 2024).

TABLE 1. Variations in the composition of MT membrane copolymers

| No | MMA (mg) | THFA (mg) | KTpClPB (mg) | HDDA (µL) | DMPP (mg) |
|---|---|---|---|---|---|
| 1 | 10 | 90 | 1 | 1 | 1 |
| 2 | 20 | 80 | 1 | 1 | 1 |
| 3 | 30 | 70 | 1 | 1 | 1 |
| 4 | 40 | 60 | 1 | 1 | 1 |

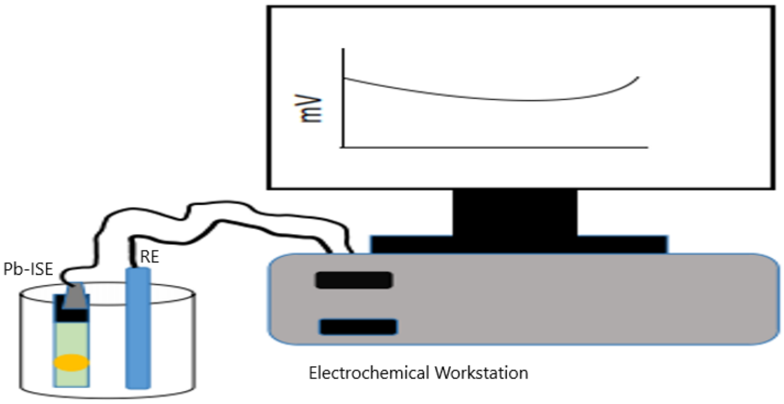

FIGURE 1. The experimental setup for $Pb^{2+}$-ISE measurements was carried out using an electrochemical workstation

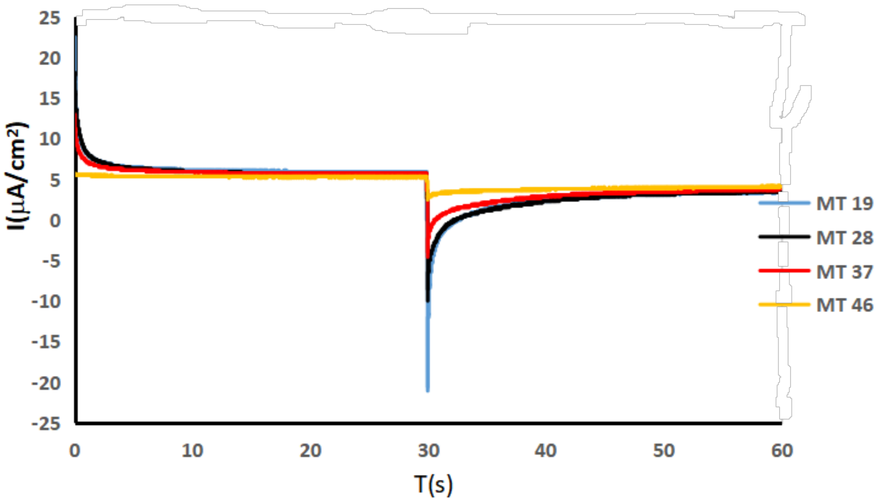

FIGURE 2. Chronoamperometry graph of MT copolymer composition variations (MT 46 = yellow line, MT28 = black line, MT37 = red line and MT19 = blue line)

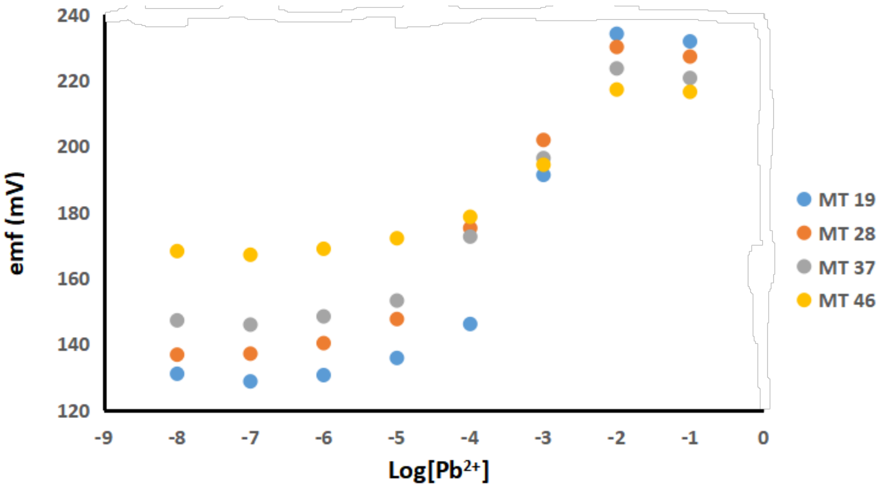

FIGURE 3. Response of MT copolymer variations to different concentrations of $Pb^{2+}$ solution

TABLE 2. Performance of MT co-polymer variations in $Pb(NO_3)_2$ solution

| Co-polymer | D ($cm^2/s$) | Slope (mV/dec) | Linear range (M) | $r^2$ |
|---|---|---|---|---|
| MT 19 | $1.51 \times 10^{-8}$ | 44.0 | $10^{-2}$ -$10^{-4}$ | 0.9998 |
| MT 28 | $1.05 \times 10^{-8}$ | 27.4 | $10^{-2}$ -$10^{-5}$ | 0.9999 |
| MT 37 | $6.52 \times 10^{-9}$ | 23.5 | $10^{-2}$ -$10^{-5}$ | 0.9945 |
| MT 46 | $1.20 \times 10^{-9}$ | 19.3 | $10^{-2}$ -$10^{-4}$ | 0.9892 |

This cannot be separated from the large amount of THFA compared to other MT copolymers. This, makes MT 19 more flexible than the other three types of MT. Due to this condition, $Pb^{2+}$ ions from the sample phase that are diffused into the membrane phase become extremely numerous. This makes the potential changes that occur on the surface of the Ag/AgCl transducer even greater (Egorov, Novakovskii & Zdrachek 2017; Gao et al. 2024). Meanwhile, in MT 37 and MT 46, the Nernstian number is found in the sub-Nernstian (< 24.6 mV/dec), especially in MT46 with a value of only 19.3 mV/dec. This is inseparable from the increasing number of MMA, which has an impact on the membrane having a higher $T_g$ value and being more rigid than MT28 and MT 19 (Azzahari et al. 2014). This condition causes the ability of $Pb^{2+}$ -ions to diffuse into the membrane to decrease by 37.9% and 88.6%, where the diffusion coefficient of MT28 co-polymer is $1.05 \times 10^{-8}$ $cm^2/s$. The MT28 copolymer in this study obtained the best Nernstian number of 27.4 mV/dec. The diffusion coefficient values obtained by MT 28 and MT 19 are similar to the diffusion coefficient for plasticized PVC membrane with a thickness of 200 mm, namely around $10^{-8}$ $cm^2/s$ (Linder et al. 2020; Pokhvishcheva et al. 2024; Zdrachek & Bakker 2018). Therefore, for further studies, MT 28 was selected as the membrane for Pb-ISE fabrication.

## LEAD IONOPHORE (IV) OPTIMIZATION

In an ISE such as Pb-ISE, the presence of ionophores in the membrane is quite crucial. This is inseparable from the function of the ionophore, which recognizes target ions that diffuse into the membrane and then brings target ions to the transducer surface. This condition causes the potential value of the transducer surface to change depending on the number of target ions carried by the ionosphere and reaching the transducer surface. The number of ionophores used greatly influences the number of target ions that reach the transducer surface (Fraga et al. 2023). Therefore, optimizing the ionophore used is very important to do. In this study, the ionophore used is IV, which is one of the ionophores that has been commonly used in Pb-ISE fabrication by several researchers before. The IV comes from the thioacetamide group (Xu et al. 2022). Four different compositions were used to carry out the ionophore optimization process in this study, as shown in Table 3.

Based on Figure 4 and Table 3, it can be seen that the optimum composition is the use of KTpClPb: Ionophore 1:1 with a Nernstian number of 27.8 mV/dec and a linear range of 0.1-$10^{-6}$ M. The results obtained are also an improvement from previous research similar to previous research by Alva et al. (2019), where a poly(tetrahydrofurfuryl acrylate) (pTHFA) membrane was used, resulting in a linear concentration range of 0.1 to $10^{-5}$ M. Meanwhile, at ratios of 2:1, 1:2 and 1:3, although the slope values close to the ideal Nernstian number of 29.6 5 mV/dec, the measurement range is shorter compared to a ratio of 1:1. At a ratio of 2:1, the resulting linear range is between $10^{-2}$ and $10^{-5}$ M, and this is similar to the response of MT28 without ionophore as shown in Table 2. This observation indicates that the lipophilic salt KTpClPB still exerts a dominant influence on the electrode response at a ratio of 2:1. This behavior can be attributed to the relatively low ionophore content, which is insufficient to effectively complex and transport $Pb^{2+}$ ions toward the transducer surface. As a result, the membrane response is governed primarily by the charge-balancing and ion-exchange properties of KTpClPB rather than by selective ion recognition, consistent with the findings reported by Aslan et al. (2023). Moreover, the amount of ionophore utilized increases at the ratio of 1:2 and 1:3. By doing this, the MT28 copolymer becomes saturated, leading to a decrease in $T_g$ of MT 28. This condition enhances the flexibility and softness of the MT28 copolymer (Cheong, Sagar & Lisak 2021). This phenomenon is closely related to the fact that increasing the amount of dissolved species within a membrane leads to a decrease in its glass transition temperature ($T_g$) (Serenko et al. 2017). Under these conditions, the components within the MT28 membrane are gradually released over time. This alters the balance of MT28's composition and decreases the response of the Pb-ISE that has been fabricated (Alva et al. 2018). Thus, MT28, which had a 1:1 ratio was selected to further perform the Pb-ISE performance study.

## Pb-ISE PERFORMANCE

In this study, the performance study of Pb-ISE involved examining its selectivity coefficient (Log $K^{Pot}_{a,b}$), pH effects, lifetime, and validation testing. The selectivity coefficient test was performed in this study using the SSM method, which is a recommended method by IUPAC

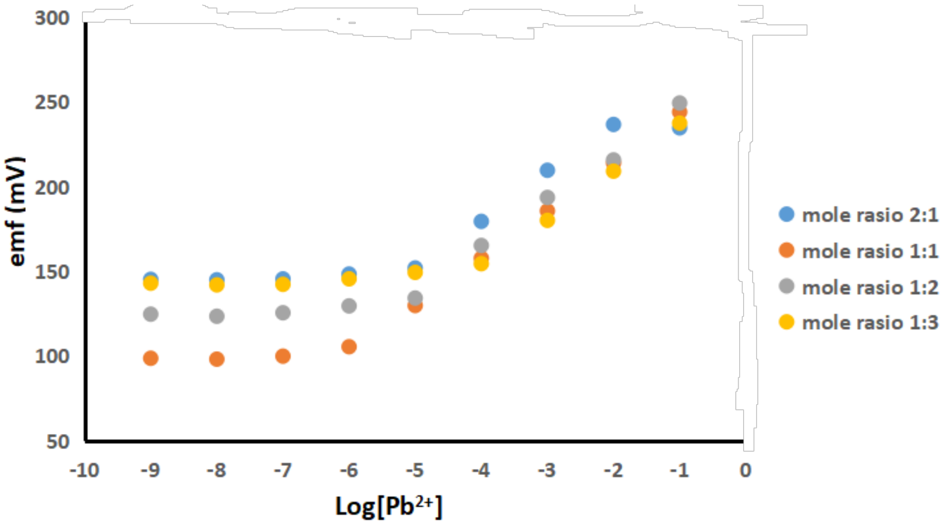

FIGURE 4. Response of MT28 variations (mole ratio of KTpClPB:Lead Ionophore) to different concentrations of $Pb^{2+}$-ions

TABLE 3. Performance of MT28 variations (mole ratio of KTpClPB:Lead Ionophore) in $Pb(NO_3)_2$ solution

| Mole Ratio | Slope (mV/dec) | Linear range (M) | LoD (M) | $r^2$ |
|---|---|---|---|---|
| 2:1 | 28.3 | $10^{-2}$ -$10^{-5}$ | $6.03 \times 10^{-6}$ | 0.9996 |
| 1:1 | 27.8 | 0.1-$10^{-6}$ | $5.37 \times 10^{-7}$ | 0.9991 |
| 1:2 | 28.1 | 0.1-$10^{-5}$ | $4.57 \times 10^{-6}$ | 0.9966 |
| 1:3 | 27.8 | 0.1-$10^{-4}$ | $5.13 \times 10^{-5}$ | 0.9993 |

(Alva et al. 2024). During the selectivity evaluation using the SSM, five interfering ions $K^+$, $Na^+$, $Mg^{2+}$, $Cd^{2+}$, and $Cu^{2+}$ were tested at a concentration of 0.1 M. The $K^+$ and $Na^+$ ions were included as interfering species because they are ubiquitous cations commonly present in environmental and aqueous samples where $Pb^{2+}$ is typically monitored. Their inclusion is essential to evaluate the selectivity of the $Pb^{2+}$-ISE and to demonstrate that the electrode response is not influenced by non-specific ion-exchange processes or background electrolyte effects caused by abundant monovalent ions. This confirms that the observed potentiometric response originates predominantly from selective $Pb^{2+}$ recognition by the membrane rather than from interference by common alkali metal ions. This selectivity coefficient test is very important to perform. The aim is to determine if Pb-ISE can perform efficiently even if there is interference from other ions (Alva et al. 2018). The selectivity coefficient test results for the fabricated Pb-ISE are shown in Table 4. The data from Table 4 shows that Pb-ISE has a selectivity that is comparable to several previous studies (Arida, Al-Haddad & Schoning 2011; Yu et al. 2011). This can be discerned in the ion selectivity coefficient (Kij) value <1 of all interfering ions (El-Alamin, Mohamed & Toubar 2022). The good selectivity coefficient of Pb-ISE is due to the difference in the radius between $Pb^{2+}$ ions and interfering ions. According to previous research, the ionophore's ability to recognize the target ion will be influenced by the ion radius size (Kabaa et al. 2018). Based on previous research reports, the size of the $Pb^{2+}$ and $Cd^{2+}$ ion radii are 1.32Å and 1.03Å (Mekatel et al. 2012). Meanwhile, the $Cu^{2+}$ ion radius is 0.73Å (Loya, Ghosh & Atta 2023), the $Mg^{2+}$ ion is 0.72Å (Bartosiewicz et al. 2022), while the $K^+$ and $Na^+$ ion radii are 1.33Å and 0.95Å (Sun 2022). Besides ion size, another factor that influences the selectivity of Pb-ISE is the use of IV which is thioacetamide, where the amide group has good binding affinity to $Pb^{2+}$ -ions (Nisah et al. 2022).

The pH effect study was carried out at pH 2 to 12, with 0.1 M $Pb(NO_3)_2$ being the test solution. The test was conducted using three different Pb-ISE sensors, and the test results can be seen in Figure 5. This pH effect test is important to do, considering that the presence of $Pb^{2+}$ ions in aqueous solutions depends on pH conditions. At acidic pH levels, Pb tends to be in an ionic state, while at basic pH levels, Pb tends to be present in the form of $Pb(OH)_2$ precipitate. This condition will have an impact on the measurement results. This is inseparable from the concept of potentiometric measurement, which measures potential changes in the concentration of an ion (Alva et al. 2024; Arida, Al-Haddad & Schoning 2011). Based on Figure 5, the potential value produced is quite stable in the pH range of 3-9. At pH 2, the potential value produced is quite high because of the protonation of the ionophore, which increases the number of cations in the MT 28 membrane. When pH is above 9, the potential value produced tends to be lower. This condition is influenced by the increasing number of $Pb^{2+}$ ions transformed into $Pb(OH)_2$, resulting in a decrease in the concentration of $Pb^{2+}$ ions in the sample solution (Alva et al. 2024).

The response of the Pb-ISE sensor used repeatedly can be seen in Figure 6. The objective of this test is to determine how much each Pb-ISE sensor can be utilized. The Pb-ISE sensor was evaluated in this study by utilizing three electrodes and a $Pb(NO_3)_2$ test solution with concentrations ranging from 0.1 to $10^{-9}$ M. The test results indicate that the Nernstian numbers of the three Pb-ISE sensors decrease with each repetition. It can be observed that the Nernstian number after the sixth measurement has already surpassed 29.6 ± 5 mV/dec. This is inseparable from the process of releasing the components contained in the MT28 membrane, which is used slowly in the sample. This causes the balance of active components in the membrane to be disturbed, and the Pb-ISE capability also decreases (Alva et al. 2024).

The final performance test is a validation test by comparing measurement results using Pb-ISE and AAS, which refer to SNI 06–6989.8-2004 for testing $Pb^{2+}$ ion samples in water. This study utilized four test samples: three artificial and one real taken from the Pesangrahan river flow (6°22′42″ S, 106°45′59″ E). This river flows close to the Cipayung-Depok final disposal site in West Java Province. The real samples used in this study were spiked using a $Pb^{2+}$ -ion solution with a concentration of 10 ppm. The validation test results are displayed in Table 5 which shows that the test between Pb-ISE and AAS yielded results equivalent to a recovery percentage of between 100.3-106.00%. This indicates that Pb-ISE can work well, with an acceptable recovery percentage value of 95 to 115% (Ata et al. 2015).

TABLE 4. Selectivity coefficient (Log $K^{pot}_{a,b}$) and $K_{ij}$ of Pb-ISE towards several interfering ions (n=3)

| Interfering Ion | $\log K^{pot}_{a,b}$ | $K_{ij}$ |
|---|---|---|
| $K^+$ | -3.70 ± 0.07 | $(1.99 \pm 0.26) \times 10^{-4}$ |
| $Na^+$ | -6.10 ± 0.07 | $(7.92 \pm 1.20) \times 10^{-7}$ |
| $Mg^{2+}$ | -12.20 ± 0.16 | $(6.58 \pm 2.40) \times 10^{-13}$ |
| $Cd^{2+}$ | -6.07 ± 0.15 | $(8.80 \pm 3.20) \times 10^{-7}$ |
| $Cu^{2+}$ | -4.23 ± 0.17 | $(6.13 \pm 2.40) \times 10^{-5}$ |

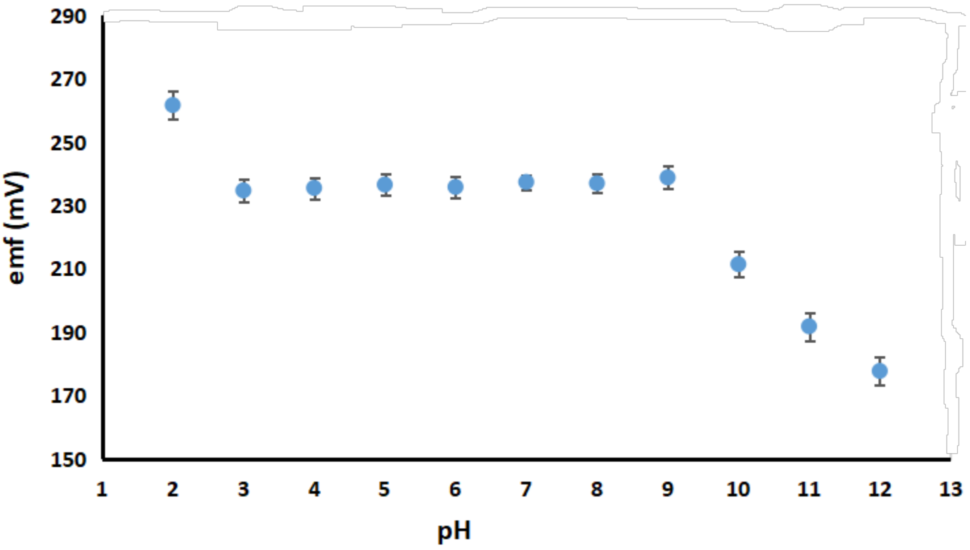

FIGURE 5. Response of Pb-ISE in 0.1 M $Pb(NO_3)_2$ solution with pH variation (2-12) conditions (n=3)

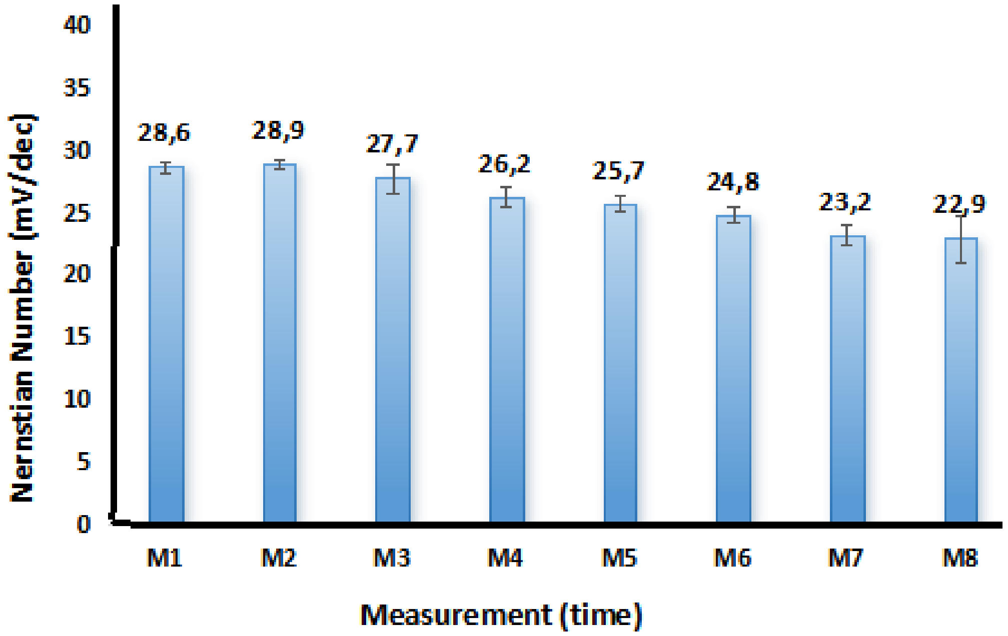

FIGURE 6. Repeated measurements of Pb-ISE responses in various $Pb^{2+}$ concentrations (n=3)

TABLE 5. Comparison of $Pb^{2+}$ -ion concentration testing between Pb-ISE versus SNI 06–6989.8-2004 (AAS methods)

| Samples | Pb-ISE | AAS | % Recovery |
|---|---|---|---|
| 0.5 ppm artificial | 0.53 ± 0.04 | 0.51 ± 0.02 | 106.0 |
| 5 ppm artificial | 5.27 ± 0.21 | 5.11 ± 0.24 | 105.4 |
| 50 ppm artificial | 52.75 ± 1.63 | 51.53 ± 2.55 | 105.5 |
| Real sample (spiking 10 ppm) | 10.03 ± 0.03 | 9.97 ± 0.09 | 100.3 |

## CONCLUSIONS

The fabrication process for Pb-ISE which is based on MT membrane has been completed successfully. This study found that MT28 was the superior MT membrane because it offered the best Nernstian number and linear range. The MT membrane also had a diffusion coefficient of $1.05 \times 10^{-8}$ $cm^2/s$. Meanwhile, MT28 with a composition ratio of KTpClPB: Lead ionophore 1:1 achieved the best performance for the fabricated Pb-ISE. The Nernstian number value achieved by MT28 with a 1:1 ratio is 27.8 mV/dec, with a linear measurement range of $0.1$-$10^{-6}$ M. The Pb-ISE that was fabricated is effective at pH levels between 3 and 9, and can be utilized up to six times. Pb-ISE also shows good selectivity towards the presence of several interfering ions such as $K^{+}$, $Na^{+}$, $Mg^{2+}$, $Cd^{2+}$, and $Cu^{2+}$. This good selectivity value can be seen from the Kij obtained, which is <1. In addition, Pb-ISE based on MT28 membranes has the same good performance as the AAS method (SNI 06-6989.8-2004), with a recovery percentage between 100.3 and 106%.

## ACKNOWLEDGEMENTS

The highest appreciation is expressed to the Directorate of Research, Technology, and Community Service, Directorate General of Higher Education, Research, and Technology, Ministry of Education, Culture, Research, and Technology, which has helped finance this research through research grant funding with Number: 105/E5/PG.02.00.PL/2024. Moreover, we express appreciation to the LPPM of Mercubuana University (LPPM-UMB) who provided operational aid through contract number 01-1-4/694/SPK/VII/2024.

## REFERENCES

Alva, S., Utami, R.S., Andrian, M., Widinugroho, A., Aziz, A.S.A., Hasbullah, S.A., Khaerudini, D.S., Feriyanto, D., Loh, K.S. & Majlan, E.H. 2024. New acrylate co-polymer membrane synthetized by photopolymerization technique for lead (II) ion-selective electrode. *Portugaliae Electrochimica Acta* 42: 337-354.

Alva, S., Suherman, R., Friliandita, V., Khaerudini, D.S., Majlan, E.H. & Aziz, A.S.A. 2020. Preliminary study of poly(tetrahydrofurfuryl acrylate) thin film as a potential material of ion selective electrodes: The case of nitrate ion-selective electrode. *Indonesian Journal of Chemistry* 20(3): 645-654.

Alva, S., Widinugroho, A., Adrian, M., Khaerudini, D.S., Pratiwi, S.E. & Aziz, A.S.A. 2019. The new lead (II) ion selective electrode based on free plasticizer film of pTHFA photopolymer. *Journal of The Electrochemical Society* 166(15): B1513-B1519.

Alva, S., Sundari, R., Aziz, A.S.A., Rashid, N.A.A. & Gunawan, W. 2018. Development of ammonium-selective electrode based on PVC/MB28 membrane. *IOP Conf. Series: Materials Science and Engineering* 453: 012042.

Arakawa, T., Dao, D.V. & Mitsubayashi, K. 2022. Biosensors and chemical sensors for healthcare monitoring: A review. *IEEJ Trans.* 17: 626-636.

Arfin, T. & Tarannum, A. 2019. Rapid determination of lead ions using polyaniline-zirconium (IV) iodate -based ion selective electrode. *Journal of Environmental Chemical Engineering* 7: 102811.

Arida, H.A., Al-Haddad, A.S. & Schoning, M.J. 2011. New solid-state organic membrane based lead-selective micro-electrode. *International Journal of Electrochemical Science* 6(9): 3858-3867.

Ariri, A., Alva, S., Khaerudini, D.S. & Aziz, A.S.A. 2022. Fabrication of lead ion selective electrodes (Pb-ISE) based on poly methyl-methacrylate-co-butyl acrylate (MB28) thin film photo-polymers and pencil graphite electrodes (PGEs). *Portugaliae Electrochimica Acta* 40: 305-323.

Aslan, N., Kocak, Z., Elif Kormalı Ertürün, H. & Sen, N. 2023. Analysis of copper(II) ions in human blood using a new solid-contact PVC membrane potentiometric sensor based on a N,N′-Bis(salicylidene)-1,3-diaminopropane Schiff base. *Analytical and Bioanalytical Research* 10(2): 193-204.

Ata, S., Wattoo, F.H., Ahmed, M., Wattoo, M.H.S., Syed Ahmed Tirmizi, S.A. & Wadood, A. 2015. A method optimization study for atomic absorption spectrophotometric determination of total zinc in insulin using direct aspiration technique. *Alexandria Journal of Medicine* 51: 19-23.

Azzahari, A.D., Yahya, R., Ahmad, M.R. & Zubir, M.B. 2014. New terpolymers from n-butyl acrylate, glycidyl methacrylate and tetrahydrofurfuryl acrylate: Synthesis, characterisation and estimation of reactivity ratios. *Fibers and Polymers* 15(3): 437-445.

Baranwal, J., Barse, B., Gatto, G., Broncova, G. & Kumar, A. 2022. Electrochemical sensors and their applications: A review. *Chemosensors* 10(9): 363.

Bartosiewicz, K., Markovskyi, A., Horiai, T., Szymanski, D., Kurosawa, S., Yamaji, A., Yoshikawa, A. & Zorenko, Y. 2022. A study of $Mg^{2+}$ ions effect on atoms segregation, defects formation, luminescence and scintillation properties in $Ce^{3+}$ doped $Gd_3Al_2Ga_3O_{12}$ single crystals. *Journal of Alloys and Compounds* 905: 164154.

Cheong.Y.H., Sagar.K. & Lisak.G.2021. Evolution of electrochemical potentials mediated by lipophilic salts at the buried membrane interface of solid contact ion selective electrodes. *Sensors and Actuators B: Chemical* 349:130766.

Egorov, V.V., Novakovskii, A.D. & Zdrachek, E.A. 2017. Modeling of the effect of diffusion processes on the response of ion-selective electrodes by the finite difference technique: Comparison of theory with experiment and critical evaluation. *Journal of Analytical Chemistry* 72: 793-802.

El-Alamin, M.M.A., Mohamed, D.A. & Toubar, S.S. 2022. New disposable ion-selective sensors for the determination of dabigatran etexilate: The oral anticoagulant of choice in patients with non-valvular atrial fibrillation and COVID-19 infection. *Measurement* 198: 111406.

Fijalkowska, G., Karpisz, K.S. & Wisniewska, M. 2020. Anionic polyacrylamide influence on the lead(II) ion accumulation in soil - the study on montmorillonite. *Journal of Environmental Health Science and Engineering* 18: 599-607.

Fraga, A.R.L., Hernandez, M.P., Garcia, A.M.D., Portales, M.V. & Hernandez, O.E. 2023. 3,3-Disubstituted 1-acylthioureas as ionophores for Pb(II)-ion selective electrodes: Physical and chemical characterization of the sensing membranes. *Phosphorus, Sulfur, and Silicon and the Related Elements* 198(5): 403-416.

Gao, L., Tian, Y., Gao, W. & Xu, G. 2024. Recent developments and challenges in solid-contact ion-selective electrodes. *Sensors* 24(13): 4289.

Ghoochani, S., Hadiuzzaman, M., Mirza, N., Brown, S.P. & Salehi, M. 2023. Effects of water chemistry and flow on lead release from plastic pipes versus copper pipes, implications for plumbing decontamination. *Environmental Pollution* 337: 122520.

Gordo, C.O., Rosales, J., Lizarraga, P., Barclay, F., Okamoto, T., Papoulias, D.M., Espinosa, A., Martinez, M.O., Kogevinas, M. & Astete, J. 2021. Blood lead levels in indigenous peoples living close to oil extraction areas in the Peruvian Amazon. *Environment International* 154: 106639.

Hajduk, B., Bednarski, H., Jarka, P., Janeczek, H., Godzierz, M. & Tanski, T. 2021. Thermal and optical properties of PMMA films reinforced with $Nb_2O_5$ nanoparticles. *Scientific Reports* 11: 22531.

Hardi, M., Siregar, Y.I., Anita, S. & Ilza, M. 2019. Determination of heavy metals concentration in produced water of oil field exploration in siak regency. *IOP Conf. Series: Journal of Physics: Conf. Series* 1156: 012009.

Iqbal, A., Jan, M.R. & Shah, J. 2021. Recovery of cadmium, lead and nickel from leach solutions of waste electrical and electronic equipment using activated carbon modified with 1-(2-pyridylazo)-2-naphthol. *Hydrometallurgy* 201: 105570.

Kabaa, E.A., Ahmed, N.M., Abdulateef, S.A. & Wahab, H.A. 2018. Determination of selectivity coefficients of sodium and potassium ion-selective electrode using porous silicon N-type (100) based extended gate field effect transistor. *IOP Conf. Series: Journal of Physics: Conf. Series* 1083: 012022.

Karatepe, A., Yemen, M., Kayapa, F., Yılmaz, E., Karipcin, F. & Soylak, M. 2022. Vortex-assisted restricted access-based supramolecular solvent microextraction of trace Pb(II) ions with 4-(benzimidazolisonitrosoacetyl)biphenyl as a complexing agent before microsampling flame AAS analysis. *Talanta* 248: 12365.

Khaerudini, D.S., Rahman, F. & Alva, S. 2020. Optimization strategy of Ag/AgCl thin film electrodes approached by chlorination process for electrochemical response materials. *Materials Chemistry and Physics* 240: 122294.

Linder, E., Guzinski, M., Pendley, B. & Edward Chaum, E. 2020. Plasticized PVC membrane modified electrodes: Voltammetry of highly hydrophobic compounds. *Membranes* 10(9): 202.

Li, J.X., Sun, C.J., Zheng, L., Jiang, F.H., Yin, X.F., Chen, J.H. & Wang, X.R. 2016. Determination of lead species in algae by capillary electrophoresis-inductively coupled plasma-mass spectrometry. *Chinese Journal of Analytical Chemistry* 44: 1659-1664.

Li, W., Zhu, Z., Chen, Q., Li, J. & Tu, M. 2023. Device fabrication and sensing mechanism in metal-organic framework-based chemical sensors. *Cell Reports Physical Science* 4: 101679.

Liu, Y., Zeng, X., Waterhouse, G.I.N., Jiang, X., Zhang, Z. & Yu, L. 2021. Potential stability improvement in $Pb^{2+}$ ion selective electrodes by applying hydrophobic polyaniline as ion-to-electron transducer. *Synthetic Metals* 281: 116898.

Loya, M., Ghosh, S. & Atta, A.K. 2023. A review on dual detection of $Cu^{2+}$ and $Ni^{2+}$ ions by using single fluorometric and colorimetric organic molecular probes. *Journal of Molecular Structure* 1278: 134949.

Megarajan, S., Kanth, K.R. & Anbazhagan, V. 2020. Highly selective rapid colorimetric sensing of $Pb^{2+}$ ion in water samples and paint based on metal induced aggregation of N-decanoyltromethamine capped gold nanoparticles. *Spectrochimica Acta Part A: Molecular and Biomolecular Spectroscopy* 23: 118485.

Mekatel, H., Amokrane, S., Benturki, A. & Nibou, D. 2012. Treatment of polluted aqueous solutions by $Ni^{2+}$, $Pb^{2+}$, $Zn^{2+}$, $Cr^{+6}$, $Cd^{+2}$ and $Co^{+2}$ Ions by Ion exchange process using faujasite zeolite. *Procedia Engineering* 33: 52-57.

Muhammad, N., Zhang, Y., Asif, M., Khan, M.F.S., Intisar, A., Mingli, Y., Subhani, Q., Cui, H. & Zhu, Y. 2020. Feasibility of pyrohydrolysis and extended-steam distillation method for the extraction of two halides from zinc and lead concentrate samples followed by ion chromatography analysis. *Microchemical Journal* 159: 105593.

Nor Farhana Nazarudin, Mohd Adam Mohd Noor, Nora'zah Abdul Rashid, Gunawan Witjaksono & Nazrul Anuar Nayan. 2014. Characterization of acrylate-based ChemFET sensor for nitrate sensing and monitoring. *IEEE Conference on Biomedical Engineering and Sciences (IECBES)*, Kuala Lumpur, Malaysia. pp. 154-158.

Nisah, K., Rahmi, R., Ramli, M., Idroes, R., Alva, S., Iqhrammullah, M. & Safitri, E. 2022. Optimization of castor oil-based ion selective electrode (ISE) with active agent 1,10-phenanthroline for aqueous $Pb^{2+}$ analysis. *Membranes* 12(10): 987.

Pokhvishcheva, N.V., Vanin, A.A., Vovk, M.A., Peshkova, M.A. & Ievlev, A.V. 2024. Application of pfg NMR diffusometry to study diffusion and ionization phenomena in plasticized polymeric membranes doped with ionic liquids. *Journal of Molecular Liquids* 403: 124874.

Saleh, T.A. & Fadillah, G. 2023. Green synthesis protocols, toxicity, and recent progress in nanomaterial-based for environmental chemical sensors applications. *Trends in Environmental Analytical Chemistry* 39: e00204.

Serenko, O.A., Roldughin, V.I., Askadskii, A.A., Serkova, E.S., Strashnov, P.V. & Shifrina, Z.B. 2017. The effect of size and concentration of nanoparticles on the glass transition temperature of polymer nanocomposites. *RSC Advances* 7: 50113-50120.

Smirnova, S.V., Mikheev, I.V. & Apyari, V.V. 2024. Aqueous two-phase system based on benzethonium chloride and sodium dihexyl sulfosuccinate for extraction and ICP-OES determination of heavy metals. *Talanta* 269: 125504.

Sun, L. 2022. Calculations of individual ionic activity coefficients of chloride salt in aqueous solutions. *Journal of Molecular Liquids* 349: 118123.

Udos, W., Ooi, C.W., Lim, K.S., Yusof, Y., Low, M.L., Zakaria, R., Wong, W.R. & Ahmad, H. 2023. Surface plasmon sensor for lead ion ($Pb^{2+}$) detection using graphene oxide – gold coated tilted fiber Bragg grating. *Results in Optics* 12: 100502.

Wang, G., Sun, D., Liang, L., Wang, G. & Ma, J. 2023. Highly sensitive detection of trace lead ions concentration based on a functional film-enhanced optical microfiber sensor. *Optics & Laser Technology* 161: 109171.

Wodyk, S., Wieczorek, M., Witaszek, P. & Poliszkiewicz, R. 2023. Design and control of the hybrid lithium-ion/lead–acid battery. *Energy Reports* 9: 106-115.

Xu, K., Liu, Y., Crespo, G.A. & Cuartero, M. 2022. Ultrathin ion-selective membranes for trace detection of lead, copper and silver ions. *Electrochimica Acta* 427: 140870.

Yagmuroglu, O. 2023. Determination of trace lead(II) in cleavers (Galium aparine) tea by UV-vis spectrophotometry after preconcentration with deep eutectic solvent/DTZ probe-based liquid-liquid microextraction. *Journal of Food Composition and Analysis* 118: 105164.

Yang, F., Yang, X., Chen, S., Hai, H., Wei, X., Wan, X., Jiao, W. & Yi, J. 2023. Label-free electrochemiluminescence sensor based on magnetic nanoparticles modified with G-quadruplex DNA for detecting lead ions. *International Journal of Electrochemical Science* 18: 100241.

Yevgeniya, O.K., Elena, G.T., Dmitry, O.K. & Konstantin, N.M. 2020. Chronoamperometric and coulometric analysis with ionophore-based ion-selective electrodes: A modified theory and the potassium ion assay in serum samples. *Sensors & Actuators: B. Chemical* 310: 127894.

Yu, S., Li, F., Yin, T., Liu, Y., Pan, D. & Qin, W. 2011. A solid-contact $Pb^{2+}$-selective electrode using poly(2-methoxy-5-(2 -ethylhexyloxy)-p-phenylene vinylene) as ion-to-electron transducer. *Analytica Chimica Acta* 702: 195-198.

Zdrachek, E. & Bakker, E. 2018. Electrochemically switchable polymeric membrane ion-selective electrodes. *Analytical Chemistry* 90(12): 7591-7599.

Zheng, T.C., Yan, F.Y., Shi, D.C., Zou, Y., Zhang, S.L. & Chen, L. 2014. Fluorescent probes for detection of lead ion. *Recent Innovations in Chemical Engineering* 7: 10-16.

*Corresponding author; email: sagir.alva@mercubuana.ac.id